RSC Advances

PAPER

View Article Online
View Journal | View Issue

Cite this: *RSC Adv.*, 2020, **10**, 27894

Rhizovagine A, an unusual dibenzo-α-pyrone alkaloid from the endophytic fungus *Rhizopycnis vagum* Nitaf22†

Ali Wang, Siji Zhao, Gan Gu, Dan Xu, Xuping Zhang, Daowan Lai * and Ligang Zhou *

Received 7th June 2020
Accepted 20th July 2020

DOI: 10.1039/d0ra05022a

rsc.li/rsc-advances

Rhizovagine A (**1**), a novel dibenzo-α-pyrone alkaloid with an unprecedented 5/5/6/6/6 fused pentacyclic skeleton, was isolated from the endophytic fungus *Rhizopycnis vagum* Nitaf22. The structure was elucidated by comprehensive spectroscopic analysis, in combination with quantum chemical ^{13}C NMR and electronic circular dichroism (ECD) calculations for configurational assignment. A plausible biosynthetic pathway for **1** was proposed. Compound **1** displayed acetylcholinesterase inhibitory activity.

Introduction

Dibenzo-α-pyrones, also known as 6*H*-dibenzo[*b*,*d*]pyran-6-ones, are a class of polyketides mainly produced by fungi.[1] Structurally, the diversity of this type of metabolites mainly arises from ring A by having different substitutions and different degrees of unsaturation, while ring B is exclusively aromatic though it might have different substituents at C-7 and C-9 (*i.e.* OMe, OH) (Fig. 1). In some unusual cases, ring A is contracted to a five-membered ring, as found in cephalosol,[2] or spiro-fused to a γ-lactone ring at C-4, as in rhizopycnolides A and B,[3] and penicilliumolide A,[4] or fused to a tetrahydrofuran, as in xinshengin,[5] or attached to a C_3 unit to form a diepoxy-cage structure, as in alternarilactone A.[6] Ring C is six-membered in all reported structures except graphislactone D that contains a seven-membered ring.[7] These metabolites display diverse biological activities, such as antimicrobial,[2,3] cytotoxic,[3,4] antioxidant,[8] and larvicidal[9] activities. The highly structural novelty as well as the interesting bioactivities made them attractive to the synthetic chemists. For example, the total synthesis of cephalosol, and graphislactones A–D has been completed.[10–12]

Rhizopycnis vagum Nitaf22 is a fungal endophyte that was isolated from *Nicotiana tabacum*, which was found to produce dibenzo-α-pyrones in our previous research,[3] as well as anisic acid derivatives.[13] In our course to searching for new bioactive fungal metabolites, this fungal strain was re-fermented in the rice medium in a large scale, which led to the isolation of a novel alkaloid, rhizovagine A (**1**) (Fig. 1). Herein, we report the isolation, structure elucidation, and the bioactivity of **1**. The biosynthetic pathway of **1** was also discussed.

Results and discussion

The fungal EtOAc extract was successively subjected to repeated column chromatography over silica gel, and ODS as well as semi-preparative HPLC to afford compound **1** (Fig. 1).

Rhizovagine A (**1**) was isolated as a minor, yellow amorphous solid. It exhibited a prominent pseudomolecular ion peak at *m*/*z* 386.1221 in the high-resolution electrospray ionization mass spectrometry (HRESIMS), indicating its molecular formula of $C_{20}H_{19}NO_7$, with 12 degrees of unsaturation. The UV spectrum displayed maximum absorptions at 203, 249, 340, and 400 nm, which were similar to the reported dibenzo-α-pyrones.[3] The ^{13}C NMR spectrum (Table 1) displayed a total of 20 resonances, which were assigned to twelve sp^2 carbons (including two sp^2 CH at δ_C 101.7, 104.7), one oxygenated quaternary sp^3 carbon (δ_C 86.2), one methine (δ_C 97.3), three methylene (δ_C 30.7, 25.4, 48.8), two methoxyl (δ_C 60.9, 55.9), and one methyl group (δ_C

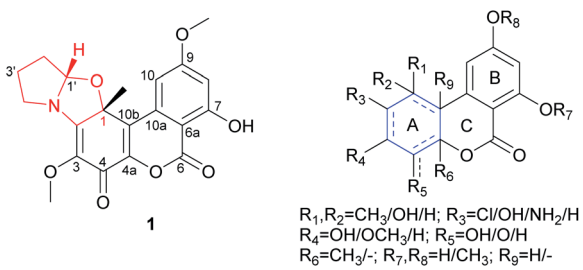

Fig. 1 Structure of rhizovagine A (**1**), and the basic skeleton of dibenzo-α-pyrones (with possible substitutions and unsaturation pattern indicated).

Department of Plant Pathology, College of Plant Protection, China Agricultural University, Beijing 100193, China. E-mail: dwlai@cau.edu.cn; lgzhou@cau.edu.cn

† Electronic supplementary information (ESI) available: ECD and ^{13}C NMR calculation data, 1D and 2D NMR, and MS spectra of **1**. See DOI: 10.1039/d0ra05022a

Table 1 ^{1}H and ^{13}C NMR data of **1** ($CDCl_3$)

Position	δ_C, type	δ_H, mult. (J in Hz)
1	86.2, C	
2	160.3, C	
3	128.7, C	
4	171.9, C	
4a	143.7, C	
6	164.4, C	
6a	100.9, C	
7	164.7, C	
8	101.7, CH	6.62, d (2.4)
9	166.6, C	
10	104.7, CH	7.20, d (2.4)
10a	134.2, C	
10b	121.7, C	
1-CH_3	26.2, CH_3	1.86, s
3-OCH_3	60.9, CH_3	3.83, s
7-OH		11.41, s
9-OCH_3	55.9, CH_3	3.91, s
1′	97.3, CH	5.65, t (5.6)
2′	30.7, CH_2	2.23, m
		1.81, m
3′	25.4, CH_2	2.11, m
4′	48.8, CH_2	3.61, m

26.2) by the aid of HSQC spectrum. Two *meta*-coupled aromatic protons (δ_H 7.20, 6.62, each d, J = 2.4 Hz) were seen in the downfield region of the ^{1}H NMR spectrum (Table 1), which were characteristic of the 7,9-dioxygenated substitutions in B ring, commonly found in dibenzo-α-pyrones.[3] One oxymethine proton (δ_H 5.65, t), and six methylene protons (δ_H 1.74–3.70) were observed in the upfield region, together with two methoxyl groups (δ_H 3.91, 3.83) and one singlet methyl group (δ_H 1.86). In addition, one chelated hydroxyl group (δ_H 11.41) was present.

The gross structure of **1** was established by extensive analysis of the 2D NMR spectra (Fig. 2). The B ring was easily constructed by analysis of the HMBC spectra. The correlations from the chelated OH (δ_H 11.41) to C-7 (δ_C 164.7), C-6a (δ_C 100.9), and C-8 (δ_C 101.7), and from the methoxyl group (δ_H 3.91) to C-9 (δ_C 166.6), allowed the assignment of a 7-hydroxyl-9-methoxyl substituted B ring. The correlations from the methyl group (δ_H 1.86, s) to C-1 (δ_C 86.2), C-2 (δ_C 160.3), and C-10b (δ_C 121.7), together with the correlation from H-10 (δ_H 7.20, d) to C-10b, clearly positioned the methyl group to C-1. The second methoxyl group (δ_H 3.83) was attached to C-3 (δ_C 128.7) as

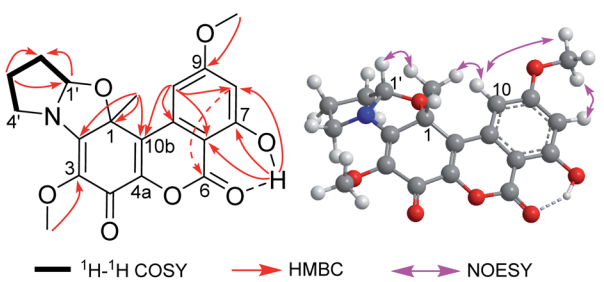

Fig. 2 Key 2D NMR correlations of **1**.

inferred from the cross-peak between them in the HMBC spectrum. Two sp^2 carbons (δ_C 171.9, 143.7) remained to be assigned, among which the former was a carbonyl group, while the latter had to be part of a double bond. By comparing the chemical shifts of these carbons with those of the co-occurring rhizopycnin B,[3] suggested that this carbonyl was located at C-4, while the other positioned at C-4a (δ_C 143.7) to complete the A and C rings.

In addition, a 2-oxygenated pyrrolidine ring was recognized by analysis of the ^{1}H–^{1}H COSY spectrum, in which correlations from H-1′ (δ_H 5.65, t) to H_2-2′ (δ_H 2.23, 1.81, m), H_2-2′ to H_2-3′ (δ_H 2.11, m), and in turn H_2-3′ to H_2-4′ (δ_H 3.61, m) were seen (Fig. 2), as well as by taken into consideration of the chemical shifts of these hydrocarbon groups, especially CH_2-4′ (δ_H 3.61/δ_C 48.8) and CH-1′ (δ_H 5.65/δ_C 97.3).[14] The above functionalities only accounted for 11 degrees of unsaturation, thus hinting the presence of one additional ring to satisfy the required unsaturation index. Then, C-1 and C-1′ had to be connected *via* an epoxy bridge, while C-2 was linked to the nitrogen atom to form a five-membered ring. This can explain the unusual downfield shift for C-1 (δ_C 86.2), comparing to that of rhizopycnin B (δ_C 69.5).[3] Moreover, the NOESY correlation between H-1′ and 1-CH_3 not only confirmed the above fusion pattern, but also defined the relative configuration of **1** (Fig. 2).

Meanwhile, in order to confirm the deduced structure, a GIAO ^{13}C NMR calculation was performed on mPW1PW91/6-311+G(2d,p)//B3LYP/6-31+G(d,p) level of theory using the reported procedure and scaling parameters.[15] As shown in Table 2, the calculated ^{13}C NMR data of the proposed structure fitted

Table 2 GIAO ^{13}C NMR calculation of **1**

Position	Exp. δ_C	Cal. δ_C[a]	$\Delta\delta$ (cal. − exp.)
1	86.2	88.0	1.8
2	160.3	161.0	0.7
3	128.7	128.4	−0.3
4	171.9	169.4	−2.5
4a	143.7	144.8	1.1
6	164.4	162.6	−1.8
6a	100.9	100.0	−0.9
7	164.7	163.0	−1.7
8	101.7	99.2	−2.5
9	166.6	164.4	−2.2
10	104.7	102.9	−1.8
10a	134.2	133.6	−0.6
10b	121.7	122.7	1.0
1-CH_3	26.2	24.8	−1.4
3-OCH_3	60.9	56.7	−4.2
9-OCH_3	55.9	53.2	−2.7
1′	97.3	96.4	−0.9
2′	30.7	31.8	1.1
3′	25.4	26.8	1.4
4′	48.8	49.9	1.1
		MAE	1.59
		RMSD	1.82

[a] Cal. δ_C was scaling corrected from calculated shielding tensor (σ) using the formula $\delta_C = (186.5242 - \sigma)/1.0533$.

well with the experimental data with MAE 1.59 ppm and RMSD 1.82 ppm. Therefore, the structure of **1** was elucidated to be a hexahydropyrrolo[2,1-*b*]oxazole fused dibenzo-α-pyrone, hitherto not reported in nature.

To determine the absolute configuration of **1**, the TDDFT ECD computations were carried out on different level of theory (pbe0/TZVP, B3LYP/TZVP, BH&HLYP/TZVP) for the B3LYP/6-31G(d)-optimized conformers of **1**. The calculated spectrum of (1*R*,1′*S*)-**1** matched the experimental data (Fig. S1, ESI†), and the best agreement was found for the BH&HLYP/TZVP-calculated one (Fig. 3), thus the absolute configuration of **1** was unambiguously assigned.

Structurally, compound **1** was characterized as one pyrrolidine fused to a dibenzo-α-pyrone uniquely *via* an oxazolidine ring. The plausible biosynthetic pathway of **1** was proposed (Scheme 1). This should involve the formation of a key metabolite, TMC-264 (**3**), which was co-isolated from the titled fungus, and was synthesized *via* the polyketide pathway.[16] This compound should be derived from alternariol (**2**) that was the first product of PKS,[17] by several tailoring steps. The nucleophilic attack from Δ^1-pyrroline that derived from L-ornithine, to the substrate **3**, would yield the iminium cation intermediate (**1a**), which then give rise to the derivative **1b** by ejecting the chloride ion (as a leaving group). The followed-up attack from 1-OH to C-1′ in **1b** should give the oxazolidine (**1**). Iminium cations were reported to be widely involved in the biosynthesis of a range of alkaloids in nature.[18,19]

Hexahydropyrrolo[2,1-*b*]oxazole or pyrrolidinooxazolidine alkaloids were not commonly found in nature. So far only 15 natural ones that incorporated in eight different skeletons have been reported, to our knowledge, which included two derivatives from the ladybird beetles, three from marine invertebrates, and ten from plants (Fig. S2, ESI†), however, none were reported from fungi. Some of these metabolites exhibited antibacterial, cytotoxic, antiplasmodial, antiviral, and phytotoxic activities,[20–23] or playing a defense role against predators.[24]

Compound **1** was thus screened for the antibacterial activity, however, it was inactive against the tested bacteria (MIC > 128 μg mL^{-1}). This compound was also tested for the antioxidant activity due to the presence of a phenolic group, whereas it did not exhibit strong activity in the DPPH radical scavenging assay

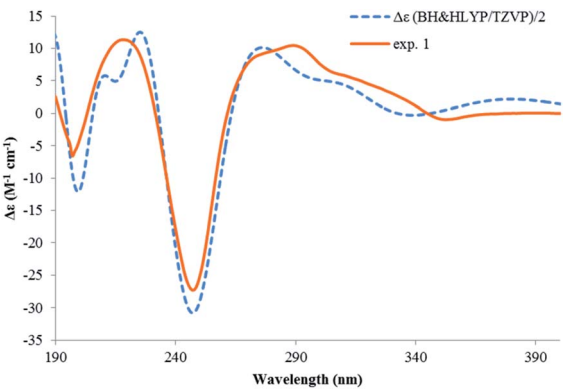

Fig. 3 Calculated and experimental ECD spectra of **1**.

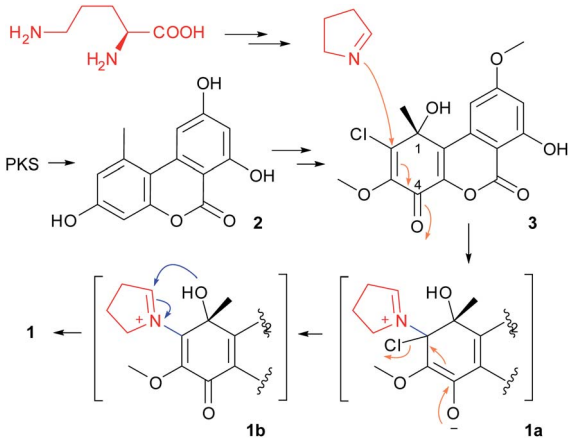

Scheme 1 Plausible biosynthetic pathway of **1**.

(IC$_{50}$ > 200 μg mL^{-1}). Meanwhile, in view of alkaloids being a major class of naturally-occurring acetylcholinesterase (AchE) inhibitors,[25] which could be of use as insecticides or a treatment for Alzheimer's disease, compound **1** was hence evaluated for its inhibitory activity against AchE. And a moderate inhibition (IC$_{50}$ 43.1 μM) was found comparing to the positive control (tacrine hydrochloride, IC$_{50}$ 6.1 μM).

Conclusions

In this study, rhizovagine A (**1**), the first fungal pyrrolidinooxazolidine alkaloid, bearing an unprecedented pentacyclic skeleton was isolated. The structure was elucidated by comprehensive spectroscopic analysis, together with quantum-chemical ^{13}C NMR and ECD calculations. Compound **1** showed AchE-inhibitory activity, which could serve as a scaffold for developing new AchE inhibitors. Moreover, due to the structural novelty, **1** could be an intriguing target for realizing a total synthesis or biosynthesis.

Experimental section

General experimental procedures

The optical rotations were recorded on a Rudolph Autopol III automatic polarimeter (Rudolph Research Analytical, Hackettstown, New Jersey). Ultraviolet (UV) spectra were recorded on a TU-1810 UV/Vis spectrophotometer (Beijing Persee General Instrument Co., Ltd., Beijing, China). Circular dichroism (CD) spectra were recorded on a JASCO J-815 CD spectrometer (JASCO Corp., Tokyo, Japan). High-resolution electrospray ionization mass spectrometry (HRESIMS) spectra were recorded on a LC 1260/Q-TOF-MS 6520 machine (Agilent Technologies, Santa Clara, CA). ^{1}H, ^{13}C, and 2D NMR spectra were measured on Bruker Avance 400 NMR spectrometers (Bruker BioSpin, Zürich, Switzerland). ^{1}H and ^{13}C NMR chemical shifts were expressed in δ (ppm) referring to the inner standard tetramethylsilane (TMS), and coupling constants in Hertz. HPLC-DAD analysis was performed on a Shimadzu LC-20A instrument equipping with a SPD-M20A photodiode array detector

(Shimadzu Corp., Tokyo, Japan) using an analytic C_{18} column (250 mm × 4.6 mm i.d., 5 μm; Phenomenex Inc., Torrance, California). Semi-preparative HPLC separation was carried out on a Lumtech instrument (Lumiere Tech. Ltd., Beijing, China) equipped with a K-501 pump (flow rate: 3 mL min^{-1}) and a K-2501 UV detector (detection was set at 370 nm) using a Luna-C_{18} column (250 mm × 10 mm i.d., 5 μm, Phenomenex Inc., Torrance, California) eluting with a mixture of MeOH and water.

Fungal material and fermentation

The endophytic fungus *Rhizopycnis vagum* Nitaf22 was isolated from *Nicotiana tabacum* previously in our lab.[3]

The fungus was cultured on potato dextrose agar for 5 days at 25 °C, and the resulting hyphae were used to inoculate 150 mL potato dextrose broth in a 250 mL flask. The culture was shaking for 7 days at 150 rpm and 25 °C, which was then used as inoculum to inoculate the autoclaved rice media in 1 L Erlenmeyer flasks each containing 100 g of rice and 110 mL of distilled water. The fermentation was carried out on a total of 10 kg of rice under static conditions at room temperature (RT) in the dark for 50 days.

Extraction and isolation

The culture was combined, dried and ground. The dry materials were extracted with EtOAc three times at RT, each for 5 days, which resulted in 163 g of extract after removal of the solvent.

The extract was subjected to vacuum liquid chromatography over silica gel (i.d. 8 cm × 30 cm) by eluting with a different mixture of petroleum ether and acetone, then CH_2Cl_2–MeOH. Fractions were pooled according to TLC, and five fractions were obtained (Frs. A–E). Fr. B was found to contain dibenzo-α-pyrones, which was then chromatographed by medium pressure liquid chromatography over silica gel using a gradient of CH_2Cl_2–MeOH (100 : 0–1 : 1, v/v) as the eluent to yield seven subfractions (Frs. B1–B7). Fr. B1 was further processed by chromatography over ODS using a gradient of MeOH/H_2O (35–100%) as the mobile phase, to afford nine further fractions (Frs. B1-1–B1-9). Among which, compound **1** (2.9 mg) was isolated from Fr. B1-5 by semi-preparative HPLC (63% MeOH/H_2O).

Rhizovagine A (1). Yellow amorphous powder; $[\alpha]_D^{25}$ +163.2 (*c* 0.125, MeOH); UV (MeOH) λ_{max} (log ε) 203 (4.57), 249 (4.66), 340 (3.86), 400 (3.84) nm; ECD ($c = 4.33 \times 10^{-4}$ M, MeOH) λ ($\Delta\varepsilon$) 218 (+11.33), 247 (−27.33), 289 (+10.46), 352 (−0.97) nm; ^{1}H NMR ($CDCl_3$, 400 MHz), ^{13}C NMR ($CDCl_3$, 100 MHz) see Table 1; HRESIMS *m*/*z* 386.1221 $[M + H]^+$ (calcd for $C_{20}H_{20}NO_7$, 386.1234).

ECD calculation

Conformational searches using Merck Molecular Force Field (MMFF) were done by the Macromodel software. Geometry optimization and frequency calculations of the MMFF-conformers using the DFT method were performed by the Gaussian 09 package.[26] TDDFT ECD calculations of the low-energized conformers (≥1%) without imaginary frequencies were carried out by Gaussian 09 using different functions (PBE0, B3LYP, BH&HLYP) and TZVP basis set with the polarizable continuum model (PCM) for MeOH. The ECD spectrum of each conformer was simulated by the program SpecDis[27] using a Gaussian band shape with an exponential half-width σ of 0.25–0.3 eV, using the dipole-length computed rotational strengths. The equilibrium population of each conformer at 298.15 K was calculated from its relative Gibbs free energies using Boltzmann statistics. The Boltzmann-averaged ECD spectrum was then generated accordingly. The generated ECD spectra were compared with the experimental one to determine the absolute configuration. The calculated ECD spectra were UV-shifted (+7, +3, and +28 nm for PBE0, B3LYP, and BH&HLYP, respectively), for comparison with the measured spectrum.

^{13}C NMR calculation

For the calculation of ^{13}C NMR chemical shifts, B3LYP/6-31+G(d,p) method was used to optimize the selected conformers. NMR calculations were performed at the level of mPW1PW91/6-311+G(2d,p) with the gauge-independent atomic orbital (GIAO) method using the SMD model for $CHCl_3$. The ^{13}C NMR chemical shifts were considered as the average value of the same atom in different conformers according to their Boltzmann distributions, using the relative Gibbs free energies as the weighting factors. The empirical scaling method was used to decrease the systematic error. The chemical shift (cal. δ_C) of each atom was scaling corrected from the calculated shielding tensor (σ) by using the formula $\delta_C = (186.5242 - \sigma)/1.0533$, using the scaling factors reported by Lodewyk, *et al.*[15] The differences $\Delta\delta$ were determined by subtracting the experimental chemical shifts ($\delta_{exp.}$) from the calculated chemical shifts ($\delta_{cal.}$). The results were evaluated in terms of the mean absolute deviation (MAE), and root mean square deviation (RMSD).

Antibacterial assay

The antibacterial activity of compound **1** was evaluated against six pathogenic bacteria, *Agrobacterium tumefaciens*, *Bacillus subtilis*, *Pseudomonas lachrymans*, *Ralstonia solanacearum*, *Staphylococcus hemolyticus*, and *Xanthomonas vesicatoria*, as described previously.[3]

DPPH radical scavenging assay

The DPPH radical scavenging activity of compound **1** was determined based on the reduction of 1,1-diphenyl-2-picrylhydrazyl (DPPH) as reported previously.[8] Butylated hydroxytoluene (BHT) was used as the positive control.

AchE inhibitory assay

The AchE inhibitory bioassay was performed using the method described by Meng *et al.*[28] Briefly, the assay was performed in 96-well plates, and in each well phosphate buffered saline (PBS, pH 7.7) solution (160 μL), AChE solution (1.0 U mL^{-1}, 10 μL), 5,5′-dithio-bis-(2-nitrobenzoic acid) solution (7.5 mM in PBS, 10 μL), and the tested compound of various concentrations (dissolved in 30% of DMSO–PBS, 10 μL) were added. After pre-incubation

at 30 °C for 15 min, 10 μL of acetylthiocholine iodide (10 mM in PBS) was added. The incubation was maintained for 30 min, then the absorbance was measured at 405 nm using a microplate spectrophotometer. Tacrine hydrochloride was used as the positive control, while PBS as the negative control. The percentage (%) of inhibition was determined using the following expression: $[(A_c - A_t)/A_c] \times 100$, where A_c is the absorbance of the negative control ($n = 3$), while A_t is that of the tested compounds ($n = 3$). The median inhibitory concentration (IC_{50}) was calculated using the linear regression between the inhibitory probability and concentration logarithm.

Conflicts of interest

There are no conflicts to declare.

Acknowledgements

Financial support for this research was provided by the National Key R&D Program of China (No. 2017YFD0201105 and 2017YFC1600905).

Notes and references

1 Z. Mao, W. Sun, L. Fu, H. Luo, D. Lai and L. Zhou, *Molecules*, 2014, **19**, 5088–5108.
2 H. W. Zhang, W. Y. Huang, J. R. Chen, W. Z. Yan, D. Q. Xie and R. X. Tan, *Chem.–Eur. J.*, 2008, **14**, 10670–10674.
3 D. Lai, A. Wang, Y. Cao, K. Zhou, Z. Mao, X. Dong, J. Tian, D. Xu, J. Dai, Y. Peng, L. Zhou and Y. Liu, *J. Nat. Prod.*, 2016, **79**, 2022–2031.
4 C. Darsih, V. Prachyawarakorn, S. Wiyakrutta, C. Mahidol, S. Ruchirawat and P. Kittakoop, *RSC Adv.*, 2015, **5**, 70595–70603.
5 F. Ye, G.-D. Chen, J.-W. He, X.-X. Li, X. Sun, L.-D. Guo, Y. Li and H. Gao, *Tetrahedron Lett.*, 2013, **54**, 4551–4554.
6 J.-W. Tang, H.-C. Xu, W.-G. Wang, K. Hu, Y.-F. Zhou, R. Chen, X.-N. Li, X. Du, H.-D. Sun and P.-T. Puno, *J. Nat. Prod.*, 2019, **82**, 735–740.
7 T. Tanahashi, M. Kuroishi, A. Kuwahara, N. Nagakura and N. Hamada, *Chem. Pharm. Bull.*, 1997, **45**, 1183–1185.
8 J. Tian, L. Fu, Z. Zhang, X. Dong, D. Xu, Z. Mao, Y. Liu, D. Lai and L. Zhou, *Nat. Prod. Res.*, 2017, **31**, 387–396.
9 Z. Mao, D. Lai, X. Liu, X. Fu, J. Meng, A. Wang, X. Wang, W. Sun, Z. L. Liu, L. Zhou and Y. Liu, *Pest Manage. Sci.*, 2017, **73**, 1478–1485.
10 Y. Xie, N. Wang, B. Cheng and H. Zhai, *Org. Lett.*, 2012, **14**, 3–5.
11 A. Arlt and U. Koert, *Synthesis*, 2010, **2010**, 917–922.
12 H. Abe, K. Nishioka, S. Takeda, M. Arai, Y. Takeuchi and T. Harayama, *Tetrahedron Lett.*, 2005, **46**, 3197–3200.
13 A. Wang, P. Li, X. Zhang, P. Han, D. Lai and L. Zhou, *Molecules*, 2018, **23**, 591.
14 W.-L. Chen, L.-Y. Wang and Y.-J. Li, *Eur. J. Org. Chem.*, 2020, **2020**, 103–107.
15 M. W. Lodewyk, M. R. Siebert and D. J. Tantillo, *Chem. Rev.*, 2012, **112**, 1839–1862.
16 M. Sakurai, M. Nishio, K. Yamamoto, T. Okuda, K. Kawano and T. Ohnuki, *Org. Lett.*, 2003, **5**, 1083–1085.
17 Y.-H. Chooi, M. J. Muria-Gonzalez, O. L. Mead and P. S. Solomon, *Appl. Environ. Microbiol.*, 2015, **81**, 5309.
18 T. Hemscheidt, in *Biosynthesis: aromatic polyketides, isoprenoids, alkaloids*, ed. F. J. Leeper and J. C. Vederas, Springer Berlin Heidelberg, Berlin, Heidelberg, 2000, pp. 175–206, DOI: 10.1007/3-540-48146-x_4.
19 T. Hartmann and D. Ober, in *Biosynthesis: aromatic polyketides, isoprenoids, alkaloids*, ed. F. J. Leeper and J. C. Vederas, Springer Berlin Heidelberg, Berlin, Heidelberg, 2000, pp. 207–243, DOI: 10.1007/3-540-48146-x_5.
20 M. Tadesse, J. Svenson, M. Jaspars, M. B. Strom, M. H. Abdelrahman, J. H. Andersen, E. Hansen, P. E. Kristiansen, K. Stensvag and T. Haug, *Tetrahedron Lett.*, 2011, **52**, 1804–1806.
21 J. H. Cardellina, R. L. Hendrickson, A. A. Stierle and G. E. Martin, *Tetrahedron Lett.*, 1991, **32**, 2347–2350.
22 Z.-X. Hu, H.-Y. Tang, J. Guo, H. A. Aisa, Y. Zhang and X.-J. Hao, *Tetrahedron*, 2019, **75**, 1711–1716.
23 G. Komlaga, G. Genta-Jouve, S. Cojean, R. A. Dickson, M. L. K. Mensah, P. M. Loiseau, P. Champy and M. A. Beniddir, *Tetrahedron Lett.*, 2017, **58**, 3754–3756.
24 P. Radford, A. B. Attygalle, J. Meinwald, S. R. Smedley and T. Eisner, *J. Nat. Prod.*, 1997, **60**, 755–759.
25 P. J. Houghton, Y. Ren and M.-J. Howes, *Nat. Prod. Rep.*, 2006, **23**, 181–199.
26 M. J. Frisch, G. W. Trucks, H. B. Schlegel, G. E. Scuseria, M. A. Robb, J. R. Cheeseman, G. Scalmani, V. Barone, B. Mennucci, G. A. Petersson, H. Nakatsuji, M. Caricato, X. Li, H. P. Hratchian, A. F. Izmaylov, J. Bloino, G. Zheng, J. L. Sonnenberg, M. Hada, M. Ehara, K. Toyota, R. Fukuda, J. Hasegawa, M. Ishida, T. Nakajima, Y. Honda, O. Kitao, H. Nakai, T. Vreven, J. A. Montgomery Jr, J. E. Peralta, F. Ogliaro, M. Bearpark, J. J. Heyd, E. Brothers, K. N. Kudin, V. N. Staroverov, T. Keith, R. Kobayashi, J. Normand, K. Raghavachari, A. Rendell, J. C. Burant, S. S. Iyengar, J. Tomasi, M. Cossi, N. Rega, J. M. Millam, M. Klene, J. E. Knox, J. B. Cross, V. Bakken, C. Adamo, J. Jaramillo, R. Gomperts, R. E. Stratmann, O. Yazyev, A. J. Austin, R. Cammi, C. Pomelli, J. W. Ochterski, R. L. Martin, K. Morokuma, V. G. Zakrzewski, G. A. Voth, P. Salvador, J. J. Dannenberg, S. Dapprich, A. D. Daniels, O. Farkas, J. B. Foresman, J. V. Ortiz, J. Cioslowski, and D. J. Fox, *Gaussian 09, Revision B.01*, Gaussian, Inc., Wallingford CT, 2010.
27 T. Bruhn, A. Schaumloeffel, Y. Hemberger and G. Bringmann, *Chirality*, 2013, **25**, 243–249.
28 X. Meng, Z. Mao, J. Lou, L. Xu, L. Zhong, Y. Peng, L. Zhou and M. Wang, *Molecules*, 2012, **17**, 11303–11314.

